We thank referee's efforts in reviewing our manuscript. Following are the replies to the comments and changes in the manuscript:

Response to referee comments #1 :

Comment 1. Identification of BB2 needs more evidence. As indicated in Figure 1, f_{60} is very close to that during the background period. Also, the back trajectory analysis in supplementary did not show a strong influence of biomass burning on the sampling site.
Reply According to the analysis of this study and Zheng's(2017), the sampling site was influenced by oxidative biomass burning particles during BB2. The decisive evidence in identifying BB2 is the elevated concentration of BC, from 115 ng to around 500 ng at night of April 5th. On the fire map, several, if not a lot, fire spots appeared around the start and middle of the back trajectory of BB2. The f60 ratio showed several peaks (> 1%) during BB2 period, and the average was 0.61% slightly higher than that during background period (0.40%).
Changes in manuscript. More evidence was added in Section 3.3.1 for identification of BB2. (Line 398-402 in marked up version, Line 355-359 in revised version).

Comment 2. While discussing the average particle number size distributions, could the authors show the average PNSD during NPF events and non-NPF events. As shown in Figure 1, the three NPF events show very high concentrations of particles between 3 – 25 nm, which are rarely seen during non-NPF days.
Changes in manuscript. One figure was added in the supplementary, showing the averaged PNSD during NPF events and the non-NPF event periods. To eliminate the influences from biomass burning, another average PNSD during the periods without either NPF events or biomass burning influences was included. The differences between the those PNSDs were discussed added in section 3.4.1 and section 3.4.2 (Line 553-559, 591-593 in marked up version, Line 491-497, 527-529 in revised version).

Comment 3. Please describe the instruments for measuring gaseous species, e.g., SO_2, CO, NO, NO_x etc. Because the concentrations of several gaseous species are very low (e.g., < 0.3 ppb for SO_2), the measurement uncertainties could be large.
Changes in manuscript. Description and uncertainty of trace gas detection was added in section 2.2 (Line 128-138 in marked up version, Line 127-136 in revised version).

Comment 4. Some analysis in this work can be more robust by incorporating the HR-ToF-AMS data which is published in Zheng et al. (2017) from the same group.
Changes in manuscript. More evidences in identifying the BB events were taken from that AMS data set in section 3.3.1 (Line 398-402 in marked up version, Line 355-359 in revised version).

Comment 5. Suggest adding "number" in the title, which is "Particle number size distribution".
Changes in manuscript. Title was changed following the comment.

Comment 6. Line 635, this study did not provide vertical profile of particles.
Changes in manuscript. This sentence was changed as "Our study provided important dataset in vertical profile of particles physical properties at Tibet Plateau." (Line 664-665 in marked up version, Line 594 in revised version)

Comment 7. The results can also be compared with another mountain site (3295 m, ASL) in Tibet Plateau (Du et al., 2015).
Changes in manuscript. Particle mass concentration, NPF frequency and particle number concentration are cited from this paper in the revised version (Table 2, Line 230, 564-565 and 613-615 in marked up version, Line 224, 503 and 549 in revised version).

Response to referee comments #2:

Comment 1. Instruments: there are two set of scanning mobility particle sizer (SMPS) and an aerodynamic particle sizer (APS) used for PNSD. When combined these data, how to deal with the overlap size range, especially for two SMPS?
Reply.
Firstly, the data from different instruments for overlap size bins didn't show big difference (Fig. R1). About how we deal with the overlap data:
1) Between two SMPS: We trust the number distribution between (3~60 nm) from the nano SMPS (DMA 3085 and CPC 3776). But the measured sample flow for CPC 3776 is very low (0.05 L/min), and the absolute number concentration has a bigger uncertainty than CPC3022 due to flow fluctuation. So we trust the absolute results from normal SMPS (DMA 3081 and CPC 3022, 0.3 L/min) at the adjacent size range. In order to eliminate the system error from flow of CPC 3776, we calculate the ratios of the particle number concentration measured by two set of SMPS within the last size bin of nano-SMPS (mean diameter at 60.4 nm). Then we use these ratios to correct the number concentration for all size bins measured by nano-SMPS.
2) Between SMPS and APS: APS data and normal SMPS data had similar value at the overlap diameter (690 nm), that over 76% data is within one order of magnitude. Considering the low number concentration in this size range and uncertainties from OPC detection and diameter transformation (from aerodynamic diameter to Stokes dimeter, assuming density as a constant) , this data set is acceptable. So we directly use the SMPS data for <700 nm part and APS data for particles larger than 700 nm in Stokes diameter.

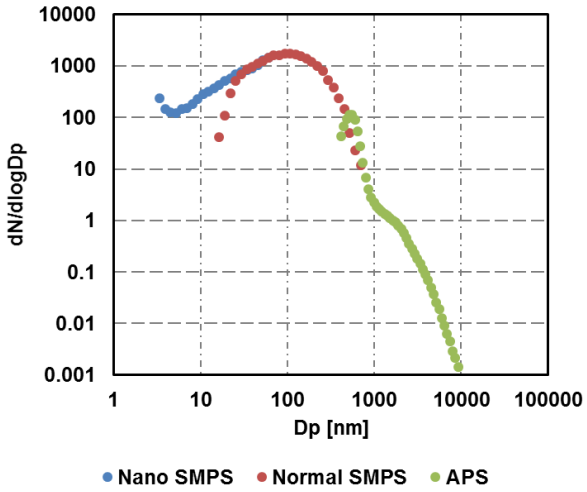

Fig R1. PNSD measured by nano SMPS (3-60 nm), normal SMPS (15-700nm) and APS (0.4-10 μm) before combined. Data were averaged for whole sampling period.

Comment 2. About backward trajectory analysis, why use different models for that, what's the difference?

Reply. The WRF model was run in Zheng et al's study (2017) for identification of biomass burning identification. HYSPLIT model was run by Dongjie Shang for analysis of new particle formation. It's just different the choices of the researchers.

Comment 3. Figure 4a, there are something wrong, the mean value is not in the range of 25-75% percentile.

Reply. We carefully checked the data , and the results are not wrong. Because mean value is not like media value, sometimes it could be outside the 25%-75% percentile, when the 0-25% or 75-100% values have big difference with other data. For this case, $N_{3\text{-}25}$ during the 3 noon of NPF days are 1-2 order of magnitude higher than other 20 days. Those data are within 75%-100%, but have a very high impact on mean value of $N_{3\text{-}25}$. So we also showed median values in order to give the another representative diurnal variation.

Comment 4. About New particle formation events: there are only three so-called NPFs during this observation period. One of them is defined by authors "Off-site NPF" during which nanoparticles were formed in PBL and transported to the site and a burst of N3-25 occurred at around 18:00, with FR at 1.64 $cm^{-3}s^{-1}$. This is contradicted. All three NPFs have different characteristics. The parameters such as FR, GR, CS may not representative for this region statistically.

Reply and changes in manuscript. We agree that only 3 individual events could not give representative NPF parameters for this region. Here in this study we want to give the case-based analysis for NPF events we observed, and try to find the key influencing factors. More multi-parameter and long-term studies are required to fully characterize the NPF events in Tibet Plateau and analyze the mechanisms behind them.

We define the third event as "off-site NPF" event, considering that the growing particle mode did not start from the lower limit of the detection (3 nm). Since 3-25 nm particles were not

formed on site, we no longer talked about FR for this case (Line 549, Table 4).

Comment 5. In conclusion: Such points are not discussed in the manuscript, but in the conclusion, such as "the atmosphere of Mt. Yulong exhibited a feature of strong oxidation", "Our study provided important data in vertical profile of particles at Tibet Plateau"
Reply and changes in manuscript. We apologize for the confusion. The "strong oxidation" is now changed to "stronger oxidation capacity than low attitude atmosphere", which is now described in section 3.1.1 (Line 242-244 in marked up version). "vertical profile" is now changed as "important dataset of particle physical properties" (Line 664-665 in marked up version, Line 592 in revised version).

Comment 6. The elevation of sampling site: 3140m or 3410m?
Reply. 3410m, that was a typing error and was corrected (Line 87 in marked up version).

Comment 7. Line 106: Silicon diffusion tube?
Reply. Thanks for stating that, it's now corrected in the manuscript (Line 107 in marked up version).

Response to referee comments #3 :

Comment.
The paper Wu et al., 2008 was cited. However, Wu et al. (2008) indicated that "Laboratory studies showed that mean diameters for the number size distributions of particles emitted by gasoline engines ranged from 40 nm to 80 nm" and "Their results showed that geometric mean diameters of particles emitted by all kinds of biofuels combustion were in the range from 110 nm to 200 nm." So the author should cited the emission test results for different kinds of fuels burning directly (diesel and gasoline traffic, biomass burning, coal, etc.) and re-write corresponding sentences.
Reply. Thanks for stating that. We rewrite those sentences, and cited results from emission test experiments as well as the PNSD source apportionment studies (Line 289-293 in marked up version, Line 264-270 in revised version).

Zheng, J., Hu, M., Du, Z., Shang, D., Gong, Z., Qin, Y., Fang, J., Gu, F., Li, M., Peng, J., Li, J., Zhang, Y., Huang, X., He, L., Wu, Y., and Guo, S.: Influence of biomass burning from South Asia at a high-altitude mountain receptor site in China, Atmos. Chem. Phys., 17, 6853-6864, 10.5194/acp-17-6853-2017, 2017.

Particle number size distribution and new particle formation under influence of biomass burning at a high altitude background site of Mt. Yulong (3410m) in China

Dongjie Shang[1], Min Hu[1, 2]*, Jing Zheng[1], Yanhong Qin[1], Zhuofei Du[1], Mengren Li[1], Jingyao Fang[1], Jianfei Peng[1], Yusheng Wu[1], Sihua Lu[1], Song Guo[1]*

[1]State Key Joint Laboratory of Environmental Simulation and Pollution Control, College of Environmental Sciences and Engineering, Peking University, Beijing, 100871, China

[2]Beijing Innovation Center for Engineering Sciences and Advanced Technology, Peking University, 100871, Beijing, China

* Corresponding author: E-mail address: minhu@pku.edu.cn, guosong@pku.edu.cn

Abstract

Biomass burning (BB) activities have a great impact on particle number size distribution (PNSD) in upper troposphere of Tibet-Plateau, which could affect regional and global climate. The intensive campaign for the measurement of PNSD, gaseous pollutants and meteorological parameters was conducted at Mt. Yulong, a high-altitude site (~~3140~~3410 m a. s. l.) in the southeast of Tibet Plateau during the pre-monsoon season (22 March to 15 April), when the intensive BB activities in South Asia were observed by fire maps. Long-range transport of BB pollutants could increase the accumulation mode particles in background atmosphere of Mt. Yulong. As a consequence, cloud condensation nuclei (CCN) concentration was found to be 2-8 times higher during BB periods than that during clean period. Apart from BB, variation of planet boundary layer (PBL) and new particle formation were other factors that influenced PNSD. However, only 3 NPF events (with a frequency of 14 %) were observed at Mt. Yulong. Occurrence of NPF events during clean episode corresponded with elevated PBL or transported BB pollutants. Due to lack of condensable vapors including sulfuric acid and organic compounds, the newly formed particles were not able to grow to CCN size. Our study emphasized the influences of BB on aerosol and CCN concentration in atmosphere of Tibet Plateau. These results

can improve our understanding of the variation of particle concentration in upper troposphere, and provide information for regional and global climate models.

Key words: Tibet-Plateau, particle number size distribution, biomass burning, CCN, new particle formation

1. Introduction

The aerosol particles can influence the radiation of the planet surface through scattering the sunlight, and cloud albedo by serving as cloud condensation nuclei (CCN) (IPCC, 2013). The cloud albedo effect of aerosols provides the biggest uncertainties in global climate models (IPCC, 2013), and depends strongly on number concentration and size of particles. Numerous studies concentrated on monitoring particle number size distribution (PNSD) within the planet boundary layer (PBL), where anthropogenic sources have strong impacts (Peng et al., 2014). While the particles in pristine free troposphere (FT) were rarely studied. Particles in FT mainly originated from lifting of emission within PBL by convective, frontal, and orographic lifting (Okamoto and Tanimoto, 2016), or atmospheric nucleation. Those particles have longer lifetime and could be transported in a longer distance, during which they could exchange with PBL (Shen et al., 2016;D'Andrea et al., 2016). Hence, studies on FT are important because : 1) CCN in FT could influence cloud albedo more directly compared to surface CCN; 2) FT served as a route of long-range transport of pollutants. Aircraft study is a direct way to measure the FT particles, but it is costly and can only provide data within short periods. Therefore, measurement at high mountain sites is one common method to study the FT particles and analyze the influences of pollution transport on FT (Shen et al., 2016).

Particles originated from BB in South Asia could have impacts on vast atmosphere of Tibet Plateau by transport in FT. As the highest plateau in the world, Tibet Plateau has very few anthropogenic sources, and could be taken as the continent background. However, recent studies revealed that the smoke plume in South Asia could ascend to FT, and transport to Himalayas and the mountain valley of Tibet Plateau during pre-monsoon season (Cong et al., 2015;Lüthi et al., 2015;Bukowiecki et al., 2016). During pre-monsoon season, the enhanced convection and steep pressure

gradient across the Himalaya-Gangetic region could rise the BB particles to higher altitude (Gautam et al., 2009;Adak, 2014). The particles could be transported by dry westerly, and have impacts on aerosols in Tibet Plateau region (Bonasoni et al., 2010;Chen et al., 2014). Former studies verify South Asian BB's influence in Tibet Plateau by chemical analysis of K^+, levoglucosan, etc. However, there was limited information of variation of PNSD under influence of BB. Also, there were limited studies concerning the contribution of BB to CCN in Tibet Plateau.

Except primary emissions, new particle formation (NPF) is another important source of particles in FT, but with limited measurement. According to model results, nucleation in FT contribute to 35 % of the CCN globally (Merikanto et al., 2009). Considering the level of pre-existing particles in FT is relatively low, it should provide a good condition for nucleation of the nanoparticles. As a result, NPF has been observed to happen frequently in FT, including Mt. Tai (1500m a.s.l.) (Shen et al., 2016), Mediterranean Sea (1000m-300m a.s.l.) (Rose et al., 2015), Mt. Puy de Dôme (1465 m a.s.l), Mt. Izana (2367m a.s.l.) (Rodríguez et al., 2009;García et al., 2014), Colorado Rocky Mountains (2900m a.s.l.) (Boy et al., 2008), etc. While NPF events happened less frequently at Indian foothill Himalayas (2080m) (Neitola et al., 2011). Studies at mountain sites considered that the frequency of NPF corresponded to the rise of PBL height, which could raise the concentration of anthropogenic SO_2, NH_3 and other nucleation precursors. Mechanisms of formation and the growth of nanoparticles in FT remain ambiguous (Bianchi et al., 2016), thus comprehensive measurements of PNSD as well as trace gases at high-mountain sites are necessary to provide information around this topic.

This study aimed to: 1) investigate the influence of BB from South Asia on PNSD and CCN concentration at South east of Tibet Plateau; 2) characterize the NPF at high-mountain sites. For purposes of these, a comprehensive measurement was conducted at a background site in Mt. Yulong (3410~~3140~~ m a.s.l.), during the pre-monsoon season.

2. Experiments and data analysis

2.1 Monitoring site

An intensive field campaign was conducted during 22 March to 15 April, at a high mountains site of Mt. Yulong (27.2N, 100.2E) in Southwest China and Southeast corner of Tibet Plateau, with an altitude of 3410~~140~~ m a. s. l. This site is one of national regional background sites coordinated by the Chinese Environmental Monitoring Center (CEMC), which is a remote site on the transport route of South Asian pollutants during pre-monsoon season. At the foot of the Mt. Yulong, 36 km to the south of the site is the famous Lijiang Old Town, a populated tourist place. More details of the monitoring site can be found in another paper (Zheng et al., 2017).

2.2 Instrumentation

PNSD was measured with a time resolution of 5 min, by two set of scanning mobility particle sizer (SMPS, TSI Inc., St. Paul, MN, USA) and an aerodynamic particle sizer (APS, TSI model 3321, TSI Inc., St. Paul, MN, USA). The first set of SMPS consisted of a short differential mobility analyzer (DMA, Model 3085) and an ultra-condensing particle counter (UCPC, Model 3776, flowrate 1.5 L/min) was used to measure the 3-60 nm particles. Another SMPS with long DMA (Model 3081) and normal CPC (Model 3022, flow rate 0.3 L/min) was used for measuring 60-700 nm particles. A silicon diffusion tube was placed before the SMPS, controlling the relative humidity of sampling air under 35 %. Diffusion loss and multiple charging calibration of the particles was done for SMPS data. APS with flow rate of 1 L/min was used for measuring 0.5-10 μm particles. The result of APS was modified to stokes diameter assuming the particle density to be 1.7 $\mu g/m^3$ before combining with SMPS data. A bypass flow was added before the inlet cutoff, to meet the working flow rate of the PM_{10} cyclone (16.7 L/min).

To investigate the BB influences in aerosols, a high-resolution time-of-flight aerosol mass spectrometer (HR-TOF-AMS) was deployed to measure the chemical composition of aerosols. Through this instrument, we can obtain the concentration of nitrate, sulfate, ammonium, chloride and high-resolution mass spectrum of organics,

especially the fragments of BB organic markers. Black carbon (BC) is another important marker for combustion sources. In this study, BC was measured with an aethalometer (Magee Scientific, USA, type AE31), by collecting aerosol particles on a filter stripe, and analyzing the transmission of the lights with seven wave length, from 370 to 950 nm. BC concentration was calculated as a multiple of the light absorption coefficient at 880nm, with the default mass attenuation cross sections of 16.6 m^2 g^{-1} (Fröhlich et al., 2015). To get the concentration of organic tracers of the new particle formation, an online-gas chromatography coupled with mass spectrometer and flame ionization detectors (GC-MS/FID) was used to measure the non-methane hydrocarbons (NMHCs), including benzene, toluene, monoterpene, etc.

Meteorological parameters, $PM_{2.5}$ and trace gases were also measured by online instruments during the campaign (Table S1). NO and NO_2 measurement was conducted by a commercial instrument (Thermo Electron model 42i NO-NO_2-NO_x analyzer) with Chemiluminescence technique. NO_2 was deoxidized to NO by a molybdenum catalyzer before detection. O_3 measurement was performed by ultraviolet (UV) absorption with Thermo Electron model 49i. CO was detected by an infrared spectrophotometry (Thermo Electron models 48i-TLE). SO_2 was measured by a commercial instrument (Thermo Electron models 43i-TLE) with ultraviolet fluorescence method. Due to the noise of the instrument and the quite low concentration of SO_2, the relative uncertainties of SO_2 measurement was high for data under 0.05 ppb.

2.3 Data processing

2.3.1 Backward trajectory analysis

The 48h backward trajectories of the air mass were computed at 4000 m a.s.l. (600 m above the ground of the Mt. Yulong site) by the Weather Research and Forecasting (WRF) model (version 3.61) to identify the impacts from South Asia. The fire spots were obtained from the satellite map from Moderate Resolution Imaging

Spectroradiometer (MODIS) (https://firms.modaps.eosdis.nasa.gov/firemap/). In order to characterize the air mass origin during the NPF events, the 48h backward trajectories at 600 m above the ground were calculated by NOAA HYSPLIT 4 (Hybrid Single-Particle Lagrangian Integrated Trajectory) model (Draxier and Hess, 1998).

2.3.2 Parameterization of NPF

The data of each PNSD during NPF was fitted as the sum of three or two mode lognormal distribution (Hussein et al., 2005), including the geometric mean diameter D_m, geometric standard deviation σ_m and total number concentration of each mode. During the NPF events, the growth rate (GR) was calculated as the variation of the mean diameter D_m of newly formed mode in unit internal:

$$\mathrm{GR} = \frac{\Delta D_m}{\Delta t} \quad (1)$$

Formation rate was calculated for nucleation fraction of the particles (3-25 nm), with the formula:

$$J_{3-25} = \frac{dN_{3-25}}{dt} + N_{3-25} \cdot CoagS_8 + F_{growth} \quad (2)$$

in this formula, $N_{3\text{-}25}$ is number concentration of particles within size range of 3-25 nm, $CoagS_8$ is the coagulation rate of particles with diameter of 8 nm, which is the geometric mean of 3-25 nm. The coagulation rate was calculated as:

$$\mathrm{CoagS}(D_p) = \int K\left(D_p, D_p'\right) n\left(D_p'\right) dD_p' \quad (3)$$

in which $n(D_p')$ is number concentration of particles with size of D_p', $\mathrm{K}\left(D_p, D_p'\right)$ is the coagulation coefficient between D_p and D_p' particles. During nucleation events, there were negligible particles that grew beyond 25 nm, so the last term in formula of was not included (Dal Maso et al., 2005). To quantify the limitation of NPF from pre-existing particles, the condensation sink was calculated as:

$$\mathrm{CS} = 2\pi \mathrm{D} \sum_i \beta \cdot D_i \cdot N_i \quad (4)$$

where D is the diffusion coefficient of the condensational vapor, e.g. sulfuric acid, β the transitional regime correction factor, D_i and N_i are the diameter and number

concentration of particles in class i. In calculation described above, all diameters were dry diameter directly measured from SMPS, so the coagulation and condensation sink could be underestimated.

Sulfuric acid was thought to be the most important precursor of NPF events (Sipilä et al., 2010), and could contribute to particle growth by condensation (Yue et al., 2010;Zhang et al., 2012). In this study, the content of H_2SO_4 was calculated by a pseudo-steady state method (Kulmala et al., 2001):

$$[H_2SO_4]=k \cdot [OH][SO_2]/CS \quad (5)$$

in which [OH] and $[SO_2]$ are number concentration of OH radicals and SO_2, value of k is 10^{-12} cm^3s^{-1}. [OH] was estimated by:

$$[OH] = a(JO^1D)^{\alpha}(J_{NO2})^{\beta}\frac{b[NO_2]+1}{c[NO_2]^2+d[NO_2]+1} \quad (6)$$

in which α=0.83, β=0.19, a=4.1×10^9, b=140, c=0.41, d=1.7 (Ehhalt and Rohrer, 2000). Contribution of sulfuric acid condensation to particle growth was calculated by Yue et al 's (2010) method.

2.3.3 Calculation of CCN concentration

In order to evaluate the variation of indirect climate effects of the particles at Mt. Yulong, CCN number concentration was estimated from data of PNSD and particle chemical composition. Firstly, the SNA (sulfate, nitrate, ammonium) was ion-coupled to get exact chemical compounds of the inorganic salts in particles. NH_4NO_3, H_2SO_4, NH_4HSO_4 and $(NH_4)_2SO_4$ were calculated following the formula:

$$n_{NH_4NO_3}=n_{NO_3^-},$$

$$n_{H_2SO_4}=\max(0, n_{SO_4^{2-}}-n_{NH_4^+}+n_{NO_3^-}),$$

$$n_{NH_4HSO_4}=\min(2n_{SO_4^{2-}}-n_{NH_4^+}+n_{NO_3^-}, n_{NH_4^+}-n_{NO_3^-}),$$

$$n_{(NH_4)_2HSO_4}=\max(n_{NH_4^+}-n_{NO_3^-}-n_{SO_4^{2-}}, 0),$$

where *n* is the mole number of the specific compounds (Gysel et al., 2007). Based on κ-Köhler theory and Zdanovskii–Stokes–Robinson (ZSR) mixing rule, the hygroscopic parameter of mixed particles can be calculated as (Petters and

Kreidenweis, 2007):

$$\kappa=\sum_1^n \varepsilon_m \kappa_m$$

where ε_m is the volume fraction of the composition *m* in particles, and κ_m is the hygroscopic parameter of pure composition *m*. In this research, we consider secondary inorganic ions, organics and BC as majority composition of particles, and put them into the ZSR mixing formula. The correlated parameters of the compounds we used are in table 1.

Table 1. Densities and hygroscopic parameters of the compounds used in CCN calculation

Species	NH_4NO_3	NH_4HSO_4	$(NH_4)_2SO_4$	H_2SO_4	Organics	BC
ρ (kg m^{-3})	1720	1780	1769	1830	1400	1700
κ	0.67	0.61	0.61	0.91	0.1	0

Based on κ-Köhler theory, the relationship between κ and D_c under certain supersaturation (S_c) is:

$$\kappa = \frac{4A^3}{27D_c^3 \ln^2 S_c}, \quad A = \frac{4\sigma_{s/a} M_w}{RT\rho_W}$$

in which $\sigma_{s/a}$ is the surface tension of water, M_w and ρ_W is the molecular weight and density of water respectively, R is 8.317 J • mol^{-1} • K^{-1}, T is the ambient temperature. With the κ of the particles, the critical diameter D_c of the CCN activation can be achieved with this formula. Then the number concentration of CCN can be calculated as number concentration of particles larger than D_c.

3. Results and discussion

3.1 Particle number size distribution

3.1.1 Particle and meteorology parameters

Fig.1 shows the time series of PNSD and correlating meteorological parameters. Temperature and relative humidity was 6.1±3.5 °C and 54.9±19.7 %, respectively (Fig.1b). Southeast wind was dominant during the campaign, followed by South wind

and Southwest wind. Average wind speed was 2.9±1.8 m/s (Fig S1). Most of the monitoring days were sunny, in favor of nucleation process, while short time rainfall occurred on 24, 26 March and 4, 6, 7, 8, 10, 11 April. During April 12, there was a heavy snow with the RH more than 90 %.

As a background high altitude site in TP, Mt. Yulong site revealed the feature of low particle concentration and strong oxidation capacity. On average $PM_{2.5}$ was 10.51±9.16 μg/m^3, similar with the results on Northeast slope of Tibet Plateau (Xu et al., 2014;Du et al., 2015). This result was only 1/10-1/3 of that in the atmosphere of urban and rural regions in China, indicating a background situation in Southwest China (Zheng et al., 2016). However, the $PM_{2.5}$ at Yulong background site during the monsoon season was around 3 times as that at ~~a~~ Qilian Shan Station (4180 m a.s.l.) in Northeast of Tibet Plateau (Xu et al., 2015) and at Jungfraujoch (3580 m a.s.l.), Switzerland (Bukowiecki et al., 2016), with similar altitude, indicating relatively stronger anthropogenic influence in ~~Southeast Tibet Plateau~~ in this area. During 22 to 30 March, 4 to 5 April and 11 to 12 April, particle mass concentration exceeded 10 μg/m^3, building up a pollution episode.

During the measurement, ozone level was 50.1±7.0 ppbv, similar with the results at high mountain sites in Europe (Cristofanelli et al., 2016;Okamoto and Tanimoto, 2016), higher than the results in Beijing during spring. This indicate that atmosphere at Mt. Yulong site had higher oxidation capacity for secondary transformation of pollutants. The concentration of NO_x and NO was 0.94±0.62 ppbv and 0.07±0.05 ppbv, respectively. SO_2 concentration was 0.06±0.05 ppbv, around the detection limit, showing no strong primary pollution. CO concentration was 0.22±0.07ppmv, and showed higher level during the start of the campaign (24 to 30 March), which could be resulted from the influence of BB (Fig 1d).

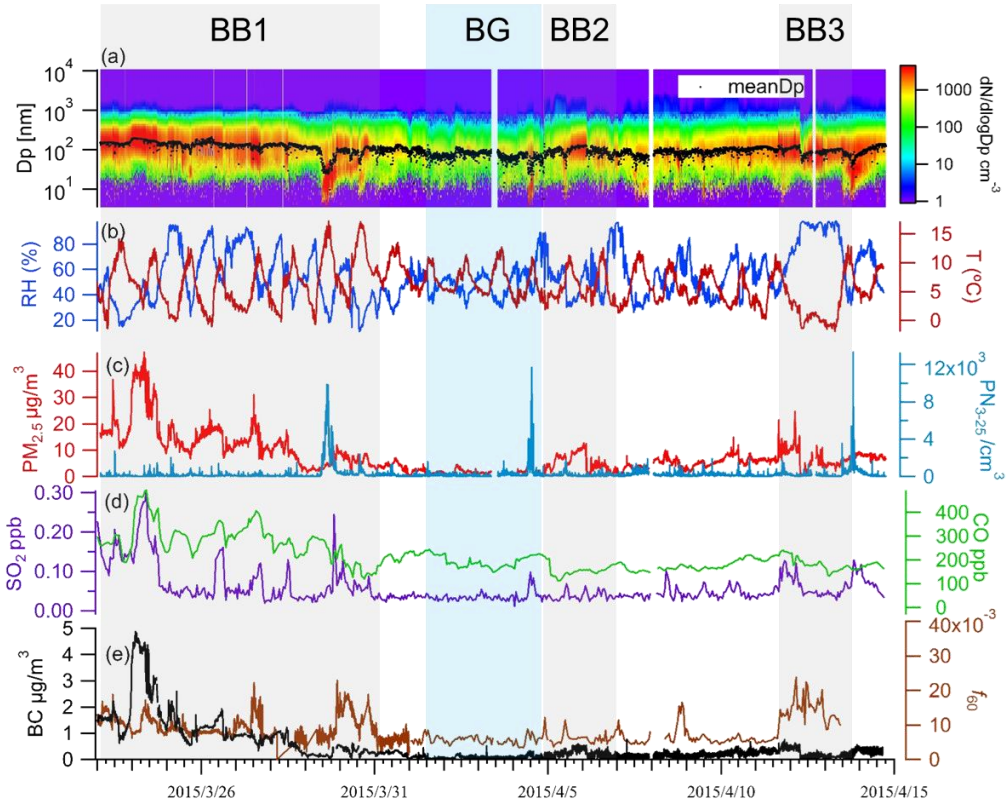

Figure 1. Time series of (a) particle number size distribution and geometric mean diameter, (b) ambient temperature, relative humidity, (c) $PM_{2.5}$ mass concentration, number concentration of nucleation mode (3-25 nm) particles (PN_{3-25}), (d) SO_2 and CO concentration, (e) black carbon concentration, fraction of *f*60 (organic fragment ions with m/z=60) during the monitoring campaign. Periods influenced by biomass burning (BB1, BB2, BB3) were marked by grey shades, period representing background condition (BG) was marked by blue shade.

Although particles we measured in this study had larger size range than most of other studies, the results can still be comparable, considering that Aitken and accumulation mode particles, which all measurements included, constitute most of the particle number concentration (PN). Table 2 showed particle number concentrations in atmosphere at Mt. Yulong and other high altitude stations. Total number concentration of PM_{10} was 1600±1290 cm^{-3} during monsoon season of Mt. Yulong, slightly lower than those measured at other sites around Tibet Plateau, e.g. Waliguan and Mukteshwar, and Mt. Huang. However, this result is several times higher than those

of areas with scarce emission sources, e.g. Alps and Antarctica. On the other hand, PN didn't show clear trend as the altitude increases, which means the regional emission and transport had larger impact on aerosols in upper troposphere, rather than the vertical distribution. We define N_{3-25}, N_{25-100}, $N_{100-1000}$, N_{1000+} as number concentrations of particles with diameters of 3-25 nm, 25-100 nm, 100-1000 nm and 1-10 μm, respectively. There were bursts of N_{3-25} on midday of 29 March, 4 April, 13 April, with the peak value at 9900 cm^{-3}, 11700 cm^{-3} and 5400 cm^{-3}, respectively (Fig.1c). During those periods, the geometric mean diameter of the particles was lower than 25 nm. Those events could be resulted from local or regional new particle formation, which would be discussed later.

Table 2. Particle number concentration of high altitude sites around the world, in comparison with this study

Location	Altitude [m]	Date	Size range [nm]	PN [cm^{-3}]	Reference
Sierra Nevada Mountains, US	1315	May-Nov 2002	10-400	4300	(Lunden et al., 2006)
Mt. Tai, China	1534	July 2010-Feb 2012	3-2500	11800±6200	(Shen et al., 2016)
Mt. Huang, China	1840	April-Aug 2008	10-10000	2350	(Zhang et al., 2016)
Mukteshwar, India	2180	Nov 2005-Nov 2008	10-800	2730	(Komppula et al., 2009)
Izana Observatory, Spain	2367	Nov 2006-Dec 2007	3-660	480-4600	(Rodr ǵuez et al., 2009)
Mt. Norikura, Japan	2770	Sep 2001, July-Sep 2002	9-300	260-1600	(Nishita et al., 2008)
University of Colorado	2900	July 2006	3-800	2881-19947	(Boy et al., 2008)

Mountain Research Station, US					
Dome C, Antarctica	3200	Spring, 2008-2009	10-600	17.9-457	(Järvinen et al., 2013)
Storm Peak Laboratory, US	3210	Mar 2012	10-10000	3100	(Yu and Hallar, 2014)
Jungfraujoch, Switzerland	3580	1995-2015	10-10000	757	(Bukowiecki et al., 2016)
Wangliguan, China	3816	Sep 2005-May 2007	12-570	2030	(Kivekäs et al., 2009)
Mt. Daban, China	3295	Sep-October 2013	12-478	2300	(Du et al., 2015)
Mt. Yulong, China	3410	May-April 2015	3-10000	1600±1290	This Study

3.1.2 Analysis of PNSD and PVSD

Average of PNSD during the measurement is showed in Fig.2a. In this study, we sorted the particles by their sizes (Dal Maso et al., 2005).– We consider that $N_{25\text{-}100}$ correlates to primary emission, and ~~P~~$N_{100\text{-}1000}$ has stronger connection with secondary formation ~~(Wu et al., 2008)~~. According to results from bench tests and road tests, gasoline and diesel vehicles will emit particles within 10–100 nm (Harris and Maricq, 2001;Kittelson et al., 2006;Benajes et al., 2017;Tan et al., 2017). While studies on source apportionment of atmospheric PNSD considered that the secondary formation or long range transport mainly contributed particles within 100-1000 nm(Wang et al., 2013b;Vu et al., 2015). The diameter with highest particle number concentration ($D_{p\text{-}max}$) was 107 nm. Number concentration (dN/dlogDp) was larger than 1000 cm^{-3} between 40-200 nm, which was the adjacent area of $N_{25\text{-}100}$ and $N_{100\text{-}1000}$. This indicates that both primary emission sources and secondary formation process had influences at Mt. Yulong site. $N_{3\text{-}25}$, $N_{25\text{-}100}$, $N_{100\text{-}1000}$ were 244 cm^{-3}, 676 cm^{-3} and 638 cm^{-3}, constituting 16 %, 43 % and 41 % of total concentration, respectively.

Different from PNSD, particle volume (PV) exhibited a bimodal distribution (Fig 2a). The first peak had an extreme value at 340 nm, representing the contribution of primary emission and aging processes. This mass peak constituted 66 % of total PV, including $PV_{25\text{-}100}$ (2 %) and $PV_{100\text{-}1000}$ (64 %). 3-25 nm particles had negligible influence on PV. Another mode in PV size distribution is within range of 1μm-10μm,

with the $D_{p\text{-}max}$ at 2.2 μm. This mode could be attributed to the suspended soil. Volume of 1-10μm particles constituted 34 % of total PV, similar with Qilian Shan station (38 %) at Northeast Tibet Plateau (Xu et al., 2015), but higher than that urban Beijing (25 %) (Wu et al., 2008), due to the much less emission sources and stronger wind at Mt. Yulong.

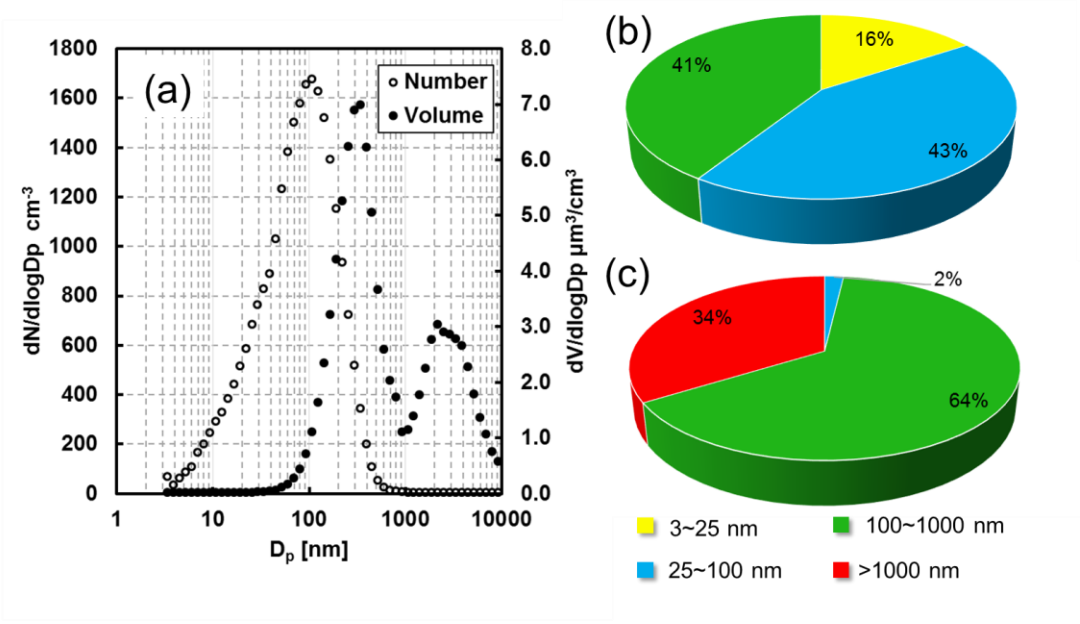

Figure 2. Particle size distribution in atmosphere at Mt. Yulong. (a) Mean size distribution of particle number (hollow circle) and volume (filled circle) concentration; Contribution of different fractions to total particle (b) number concentration and (c) volume concentration. Different colors represent different size ranges: yellow (3-25 nm), blue (25-100 nm), green (100-1000 nm), red (1-10 μm).

To better characterize the contribution from different process, the mean PNSD was fitted to three lognormal modes (Fig. 3, Table 3). We define the three fitted modes as nucleation mode, Aitken mode and accumulation mode, based on their geometric mean diameters, which were within 3-25 nm, 25-100 nm and 100-1000 nm, respectively. Nucleation mode can be derived from nucleation process. Nucleation mode contributed 15 % to total PN, which was half lower than proportion of nucleation mode particles at Mt. Tai, indicating relatively less impact from nucleation

events. Median diameter of Aitken mode and accumulation mode particles are 52 nm and 130 nm. These mean diameters are similar with the results at Jungfraujoch (Bukowiecki et al., 2016) and Beijing (Wu et al., 2008). Accumulation mode particles, correlating with secondary formation (mode_3), contributed 54 % to total PN, which is twice higher than the result in urban Beijing (Wu et al., 2008), and similar with that in pristine atmosphere of Jungfraujoch (Bukowiecki et al., 2016). This result indicates that aerosols arrived at Mt. Yulong were aged during the transport.

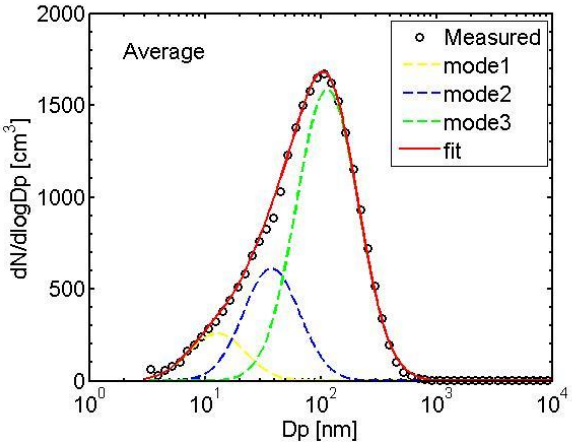

Figure 3. Lognormal fit (3 modes) of average particle number size distribution during the campaign at Mt. Yulong. Black circles mark the measured PNSD, colored dash lines represent the PNSD of fitting modes, and red full line marks the sum of PNSD of all fitting modes. Mode 1, 2 and 3 were nucleation mode, Aitken mode and accumulation mode, respectively.

3.2 Influence of PBL diurnal variation on PNSD

Figure 4 shows the diurnal variation of $N_{3\text{-}25}$, $N_{25\text{-}100}$, $N_{100\text{-}1000}$ during the sampling period. The particle number concentration in nucleation fraction and Aitken fraction showed a clear diurnal variation. Mean value of $N_{3\text{-}25}$ started to increase at 10:00 in the morning, and reached around 500 cm^{-3} at noon due to nucleation events at noon (Fig. 4a). However, the median of $N_{3\text{-}25}$ didn't showed similar diurnal variation because of low NPF frequency. On the other hand, both mean and median of

346 $N_{25\text{-}100}$ showed a local maximum during 10:00-14:00 (Fig. 4b). NPF events could not
347 cause this variation, since newly formed particles were not able to grow to 25 nm in
348 the morning. So the increased 25-100 nm particles originated from primary sources,
349 e.g. traffic sources and biomass burning. Considering that no anthropogenic emission
350 sources around the site, those primary particles could be transported from other
351 regions. During noon time, as the convection is strongest, $N_{25\text{-}100}$ could be raised by
352 the elevated urban PBL during the day, and anthropogenic particle injected during this
353 process (Tröstl et al., 2016b). Adak et al. (2014) also reported that number
354 concentration of PM_1 increased during day time, corresponding with the up-slope
355 valley wind. In the afternoon, the convection become weaker, and the larger wind
356 speed (Fig. 4e) had stronger scavenging effect on those primary particles, so $N_{25\text{-}100}$
357 decreased at around 14:00.

358 The diurnal change of absolute water content also support that Mt. Yulong site
359 was influenced by elevated PBL during midday. The water concentration was
360 calculated based on temperature and relative humidity, and showed an increase from
361 3.3 g m^{-1} to 4.2 g m^{-1} during 9:00-12:00, and descended back to 3.6 g m^{-1} till 14:00
362 (Fig. 4f). This systematic water content variation indicates that the site was influenced
363 by the PBL during day time. Shen et al (2016) used the increase of water content
364 together with Aitken mode particles, to separate the PBL conditions at Mt. Tai. The
365 value of CO/NO_y and NO_y/NO_x was used in other studies to determine the age of the
366 air masses arriving high altitude sites (Tröstl et al., 2016b;Zellweger et al.,
367 2003;Jaeglé et al., 1998). Because NO_y was not measured in this study, we used
368 CO/NO_x to estimate the age of air mass since contact with primary emission. CO/NO_x
369 was 287±146 at Mt. Yulong, lower than Jungfraujoch (Herrmann et al., 2015), Mt.
370 Cimone (Cristofanelli et al., 2016) and Kansas (Jaeglé et al., 1998), indicating a
371 stronger anthropogenic influence. The diurnal variation of CO/NO_x showed minimum
372 during 9:00-14:00 (Fig. 4d), consistent with the local maximum of water content and
373 $N_{25\text{-}100}$. The diurnal variation of O_3/NO_x exhibited a similar trend as CO/NO_x, with an
374 average of 69.6 during 10:00-14:00, and 83.6 during 1:00-6:00 (Fig. S2). Those
375 evidences indicate that at least during 10:00-14:00, Mt. Yulong site was influenced by

elevated PBL. On the other hand, we consider the data during 1:00-6:00 as the condition within FT, when $N_{25\text{-}100}$ and water content were lowest and CO/NO_x were highest. However, $N_{100\text{-}1000}$ didn't show obvious diurnal variation, indicating the elevated PBL didn't inject large amount of 100-1000 nm particles.

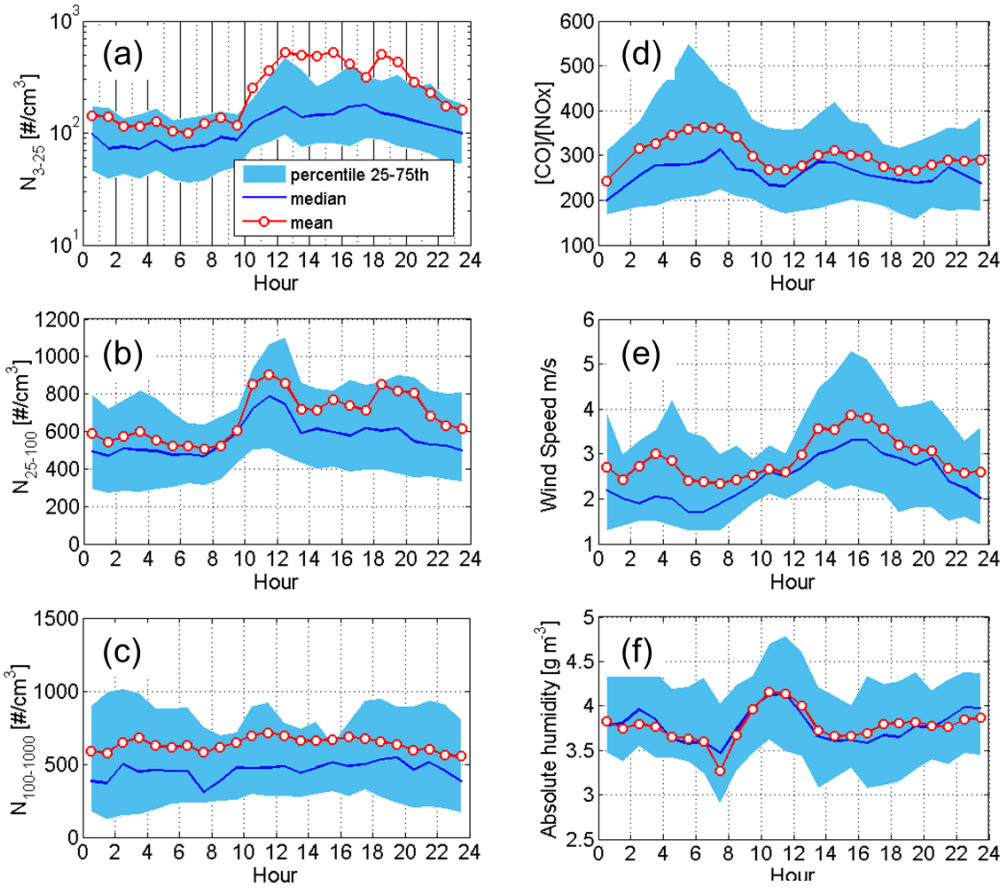

Figure 4. Diurnal variations of $N_{3\text{-}25}$, $N_{25\text{-}100}$, $N_{100\text{-}1000}$, CO/NO_x, wind speed, and absolute humidity at Mt. Yulong during monitoring campaign. Red lines with circles, blue lines mark the mean and median results, respectively. Light blue area marks the range between 25th, and 75th percentiles of the data.

3.3 Influences of BB on Mt. Yulong

3.3.1 Identification of BB episodes

Background condition (BG) was picked during 1 to 4 April, when the concentration of BC was 85 ng m^{-3} on average. During this period, the wind was relatively stronger, and fire spots were barely found on the westward path of the air

mass (Fig. S3). Based on the background condition, three BB events were identified by the following criteria: 1) BC was more than the background level (85 ng m^{-3}); 2) higher fraction of *f*60 than during BG (0.4 %); 3) fire spots appeared in the source regions of the air masses or surrounding areas of the site.

During the first BB event (BB1, 22 to 30 March), dense fire spots were found on the source region in north Burma. BC concentration (1.2 μg m^{-3}), PV and *f*60 signal showed highest level during BB1. Trajectories of BB2 (5 to 6 April) passed fewer fire spots in South Asia than BB1, and the BC concentration was lower (0.3 μg m^{-3}). Concentration of organic components during BB2 was 4 times as that during background period. According to an AMS study from the same campaign, organic particles during BB2 were mainly influenced by transported oxidized organics originated from biomass burning (OOA-BB), other than fresh BB organic aerosols (Zheng et al., 2017). The proportion of *f*60 was highest (1.4 %) during BB3 (11 to 12 April), showing strong BB influence. However, few fire spots were observed on the path of air mass, indicating the BB particles could be derived from domestic heating nearby. Zheng's study (2017) also indicated that organic aerosols showed character closer with fresh BBOA compared with BB1.

3.3.2 Influences of BB on PNSD and CCN

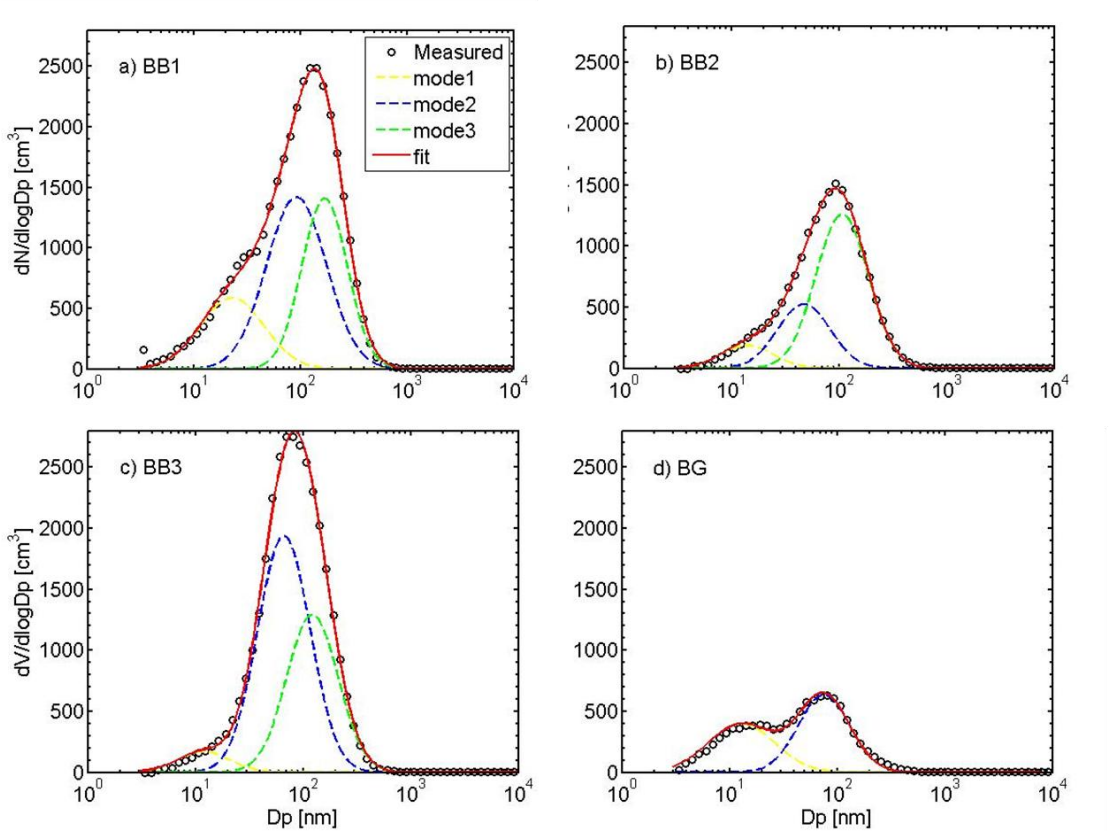

Figure 5. Lognormal fit (3 modes) of average PNSD during (a) BB1, (b) BB2, (c) BB3, (d) BG at Mt. Yulong site. Black circles mark the measured PNSD, colored dash lines represent the PNSD of fitting modes, and red full line marks the sum of PNSD of all fitting modes. Mode 1, 2, 3 were nucleation mode, Aitken mode and accumulation mode, respectively.

The average PNSDs during BB events and BG condition were plotted in Figure 5, and fitted by 3-mode lognormal distributions. The fitting results are showed in Table 3. For the BG condition, only two modes were obtained (Fig. 5d), including nucleation mode (mode_1, D_{mean} = 15 nm) originated from nucleation events and Aitken mode (mode_2, D_{mean} = 79 nm). Their total number concentration was 669 cm^{-3}, similar with the level at Swiss Jungfraujoch (Herrmann et al., 2015), exhibiting an Eurasia background character.

The averaged PNSD during those BB episodes showed discrepancies, indicating the variant influences of transported and local BB on particles in atmosphere of Mt.

Yulong. During the BB2, Aitken mode number concentration was similar with that during BG condition. But an accumulation mode (mode_3, D_{mean} = 106 nm) with higher PN (775 cm^{-3}) appeared (Fig. 5b). This mode with larger size could be the aged particles transported from BB source regions in South Asia. Different from BB2, Aitken mode particles were increased by a factor of 3 and became dominant in PNSD during BB3 the local event (Fig. 5c). The number concentration of this mode was 1309 cm^{-3}, 2 times more than accumulation mode particles. The reason could be that the particles during BB3 were freshly emitted from sources nearby the monitoring site. The study of Zheng et al (2017) also showed that during this period, the OOA fraction in organic aerosols was relatively lower, while BBOA fraction was higher, indicating impacts from more local BB sources. The geometric mean diameters of accumulation mode were 169, 106, 130 nm during BB1, BB2, and BB3, smaller than that of aged biomass burning particles at Mt. Bachelor, USA (Laing et al., 2016), indicating the particles at Mt. Yulong were more fresh. Nucleation mode had lower PN during BB2 and BB3, since the higher PN of larger particles played as strong coagulation sink of nucleation mode particles. Aitken mode and accumulation mode were comparable during BB1 (Fig. 5a), indicating the fresh aerosols from sources surrounding the site had comparable influence as the transported aged BB aerosols.

In a word, the BG condition at Mt. Yulong could represent the background level of particles of TP or even Eurasia. The local and long-range transported BB emissions would increase the level of Aitken mode and accumulation mode particles, respectively.

Table 3. Fitted parameters of lognormal modes for different period. μ, σ and N represent the mean diameter, standard deviation, and total number concentration of each mode, respectively. "Total" represents the mean result of all data achieved from the campaign.

Period	μ [nm]			σ [nm]			N [cm^{-3}]		
	mode_1	mode_2	mode_3	mode_1	mode_2	mode_3	mode_1	mode_2	mode_3
Total	16	52	130	1.75	1.75	1.77	221	488	861
BB1	23	92	169	1.94	1.91	1.63	428	1014	744

BB2	16	47	106	1.75	1.75	1.75	117	302	775
BB3	15	70	130	1.75	1.75	1.72	106	1309	628
BG	15	79	-	2.03	1.73	-	301	368	-

Concentration of CCN was calculated following method described in section 2.3.3. κ value during the sampling period was 0.12±0.01, only 1/3 from urban Beijing (Wu et al., 2016) and a rural site at Thuringia, Germany (Wu et al., 2013), but consistent with the results in Alberta, Canada (0.11±0.04) during BB events (Lathem et al., 2013). Pierce et al (2012) reported that κ was around 0.1 for >100 nm particles in a forest mountain valley during biogenic secondary organic aerosols formation and growth events. Similarly, organic volume fraction was 0.73 in particle at Mt. Yulong, explaining the low value of κ. As a result, the D_c at SS of 0.6 % and 1.2 % was 72.0±2.2 and 45.4±1.4 nm, respectively. There could be uncertainties for value of κ and D_c, since here we used a manually set hygroscopicity of organics, which may varied with oxidation level or other factors (Wu et al., 2016). Considering the variation range of D_c was small, the CCN concentration was mainly controlled by size distribution of particle number.

BB events raised the CCN level in atmosphere by influencing the PNSD. Increase of PN was observed during BB events, i.e. 2207±1388 cm^{-3}, 1214±638 cm^{-3}, 2062±1112 cm^{-3} during BB1, BB2, BB3, respectively. As a consequence, the increased particles played as CCN in atmosphere of Mt. Yulong, forming a readily increase of CCN concentration during BB events. Figure 6 showed the mean number concentration of CCN in periods under PBL influence (10:00-14:00, as discussed in 3.2) and FT condition (1:00-6:00) during BG and BB events. Mean number concentration of CCN under supersaturation of 0.6 % was 936±754 cm^{-3} and 807±705 cm^{-3} for PBL and FT periods at Mt. Yulong, comparative with boreal forest station in Finland (Cerully et al., 2011). The concentration of CCN in PBL condition during BB1, BB2, BB3 was 5, 2, 2 times as that during BG. Promotions of CCN during BB1, BB2, BB3 were more remarkable for FT, i.e. 9, 3, 8 times as BG (Fig. 6). This result indicates that the BB particles from South Asia could have strong influence on the climate parameter. For the data under supersaturation of 1.2 %, the ratios between

CCN concentration of BBs and that of BG were less, i.e. 2-4 times for periods influenced by PBL, and 2-7 times for FT conditions. This is because critical diameters under supersaturation 0.6 % and 1.2 % were around 72 nm and 45 nm, respectively. And PN within 45-72 nm was relatively stable compared to the larger particles, because of the daily input of anthropogenic primary aerosols from urban air masses.

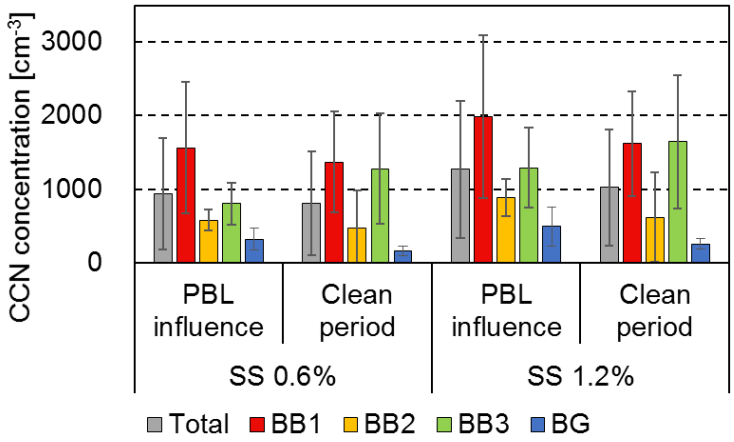

Figure 6. Mean number concentration of CCN under supersaturation of 0.6 % and 1.2 % during whole monitoring period (labelled as "total"), BB1, BB2, BB3 events (marked by shadow in Fig. 1). PBL (10:00-14:00) and FT (1:00-6:00) conditions were separated.

3.4 New particle formation events

3.4.1 NPF events at Mt. Yulong under anthropogenic influences

Following the method Tröstl et al (2016b) and Yli-Juuti et al (2009) used, we define the three NPF events on 29 March, 4 and 13 April as follows:

a) Type A event on 29 March: appearance of newly formed particles (3 nm, the first bin of nano-SMPS) and continuous growth of those particles, reaching the upper limit of nucleation mode (25 nm). This NPF event was within the period of BB1, the air mass arriving at Mt. Yulong was from North part of Burma with slow movement before 28 March, transporting abundant pollutants to this area. During 28 March 12:00 to 29 March 6:00, the air mass was from west upper troposphere

(Fig S4), cleaning out the pre-existing particles built up by BB events. CS at Mt. Yulong decreased from 0.006 s^{-1} to 0.002 s^{-1} on morning of 29 March. On the other hand, the concentration of SO_2 was stable (around 0.04 ppb) before occurrence of nucleation. The calculated H_2SO_4 increased before nucleation, reaching 5×10^6 cm^{-3} (Fig. S4). The nucleation rate was 1.43 $cm^{-3}s^{-1}$, increasing nucleation mode particles to around 10^4 cm^{-3}. Benefited by the increase of α-pinene (from 0.02 ppb to 0.10 ppb), β-pinene (from 0.03 ppb to 0.20 ppb) and SO_2 in day of 29 March, the formation of secondary aerosol continued, and the newly formed particles grew over 30 nm before night. This process could be from gaseous oxidation and condensation. Particle growth stopped during night of 29 March, when the gaseous reaction was inhibited because of absence of sunlight. After sunrise on 30 March, the particle continued growing and reached 40 nm. Concentration of toluene was lower than 0.1 ppb, indicating small contribution from anthropogenic VOCs. The GR was 3.48 nm h^{-1} within size range of 3-25 nm. In a word, under the influence of transported pollutants, nucleation was triggered by the upper clean air mass, which reduced level of pre-existing particles. While growth of particles was favored by the photochemical reaction and condensation process.

b) Type B event on 4 April: newly formed mode occurred with growing trend, but growth stopped at early stage (<15 nm), and there were temporal low values of $N_{3\text{-}25}$ during the event. The event on 4 April was under BG condition, during which concentration of SO_2 was lower (around 0.02 ppb). Started from 2:00 on 4 April, the air mass arrived at Mt. Yulong was transported by upslope flow from west lower troposphere. While during 9:00-12:00, the air mass arrived at Mt. Yulong passed Northeast India, where fire spots could be observed on the MODIS map during 2 April. Thus, the gaseous pollutants and particles from anthropogenic sources nearby or from BB sources in Northeast India was transported to this site on morning of 4 April. Concentration of SO_2 and [H_2SO_4] increased to 0.07 ppb and 6×10^6 cm^{-3} at 11:00, respectively, corresponding to occurrence nucleation (Fig.

S5). SO_2 shared similar time series with black carbon, indicating a combustion source. FR and GR were 0.93 cm^{-3} s^{-1} and 3.2 nm h^{-1}, respectively. N_{3-25} fluctuated during NPF events, showing low values when there were temporary changes in cloud condition (influencing radiation) and wind direction. Concentrations of β-pinene and Toluene were stable and lower than 0.10 ppb and 0.65 ppb respectively throughout the NPF event, which could be the reason of smaller growth rate. At around 14:00, the source region of air mass varied to west upper troposphere, and the stronger wind cleaned out both the nucleated mode particles and gaseous precursors, terminating the NPF event. In summary, type B event under background condition was triggered by the injection of gaseous pollutants from elevated PBL and short term transport of BB pollutants.

c) Off-site NPF event on 13 April: A narrow ~~Aitken mode~~ band (~~25~~8-50 nm) was observed in PNSD from 13 to 14 April. The primary particles should have wider range and larger size. These particles were mostly likely nucleated off-site, and transported to Mt. Yulong site by uplifting air mass. On the afternoon of 13 April, the air mass arrived at Mt. Yulong passed the local ground layer (yellow trajectory in Fig S6). SO_2 increased from 0.06 ppb to 0.13 ppb, and toluene reached highest level at 0.098 ppb (Fig. S6), indicating an anthropogenic impact. As a result, particles formed from the ground level were transported to the site and a burst of N_{3-25} occurred at around 18:00~~, with FR at 1.64 cm^{-3} s^{-1}~~. β-pinene also showed higher value at dawn of 13 April. Those nanoparticles showed a growth trend, with GR at 2.99 nm h^{-1}. To summarize, occurrence of nucleation mode particles were off-site nucleated in PBL and transported to this site.

The new particle formation events had strong influences on PNSD. Particles showed unimodal distribution during non-NPF event periods, with the peak diameter at around 125 nm (Fig 7S). This is mainly due to the impact from aged biomass burning particles. During those NPF events, PNSD showed a clear bimodal characteristic. The smaller mode was originated from nucleation and growth of nanoparticles. This mode had a higher peak than the larger mode, indicating that NPF

559 significantly contributed to particle number concentration.

560 3.4.2 Limiting factors of NPF events

561 Frequency of NPF was 14 % during our measurement. This NPF frequency is
562 clearly less than polluted atmosphere of North China Plain (40-65 %) in March and
563 April (Wang et al., 2013a;Shen et al., 2011), the top of Mt. Huang (38 %) during April
564 (Zhang et al., 2016), a background site in Northeast Tibet Plateau (79%) in autumn
565 (Du et al., 2015) and a remote rural site in the Sierra Nevada Mountains (47 %) in
566 spring (Creamean et al., 2011). A common knowledge is that CS is the limiting factor
567 that controls the NPF (Cai et al., 2017). Thus, pre-existing particle levels on event
568 days should be less than non-event days, at high altitude mountain sites (Shen et al.,
569 2016;Guo et al., 2012) as well as urban sites (Wang et al., 2011;Wang et al., 2017).
570 The low NPF frequency was unexpected in clean atmosphere of Mt. Yulong, since the
571 mean CS at Mt. Yulong was 0.0038 s^{-1}. On the other hand, similar low frequency of
572 NPF events were also observed in pristine atmospheres, e.g. 24 % at Antarctic site
573 Neumayer (Weller et al., 2015), 12-17 % at Dome C, Antarctica (Järvinen et al.,
574 2013).

575 During the first five days of the campaign (22 to 27 March), the nucleation
576 events could be prevented by large amount of pre-existing particles acting as big
577 condensation sink. The CS was more than 0.005 s^{-1}, similar with polluted Beijing on
578 days with NPF events (Wu et al., 2007). However, on rest of days when CS was even
579 lower than 0.002 s^{-1}, the NPF events were still scarce. Considering that the content of
580 condensable vapor participated in nucleation is determined by the competition
581 between formation from precursor oxidation and condensation on surface of
582 pre-existing particles (Zhang et al., 2012), the lower NPF frequency at pristine sites
583 could be resulted from lack of precursor, e.g. VOCs and SO_2 from fossil fuel and
584 biomass burning sources.

585 To further evaluate the effect of different parameters on NPF, daily variations of
586 SO_2, CS, $J(O^1D)$, Benzene and β-pinene during 28 March to 14 April were calculated

and plotted in Figure 7. The results during 10:00-14:00 were picked up as the occurrence time of nucleation, and compared between NPF days and non-event days. As shown in Fig. 7, NPF days and non-NPF days shared same level of $J(O^1D)$, and 15 % difference in CS when nucleation happened, indicating small influence of solar radiation and pre-existing particles on NPF. In addition to this, if we took out the data under biomass burning influences from non-NPF days, the averaged PNSD (Fig S7) was similar with the PNSD during NPF days in larger size range (> 80 nm). Considering that larger particles are the main contributor to condensation and coagulation sink, we can conclude that in the pristine atmosphere of Mt. Yulong, CS is not the decisive factor on NPF.

The concentration of SO_2 showed increase on NPF days, 60 % higher than non-event days, indicating the anthropogenic SO_2 as the controlling factor of NPF at Mt. Yulong. Studies at Jungfraujoch (Bianchi et al., 2016;Tröstl et al., 2016b), Izaña (García et al., 2014) and Mukteshwar (Neitola et al., 2011) also reported that the nucleation events in upper troposphere corresponded to increase of anthropogenic gas pollutants by elevated PBL. At Daban Mountain on the North slope of TP, the $PM_{2.5}$ level was similar with Mt. Yulong, but NPF could be observed nearly every day. It may be caused by that the SO_2 was around 2 ppb on average, two order of magnitude higher than Mt. Yulong.

Organics may also be a driven factor on NPF. The concentration of β-pinene showed higher value (40 %) in the afternoon on NPF days, while there was little difference (9 %) between NPF days and non-event days on anthropogenic benzene. Recent studies considered that apart from sulfuric acid, the highly oxidized multifunctional organics from biogenic VOCs could take part in nucleation as well as growth (Huang et al., 2016;Tröstl et al., 2016a), in free troposphere, the pure organic nucleation without sulfuric acid may even be dominant (Bianchi et al., 2016;Gordon et al., 2016). According to Du et al 's study(2015), the fraction of oxidized organics in particle phase had positive relationship with particle growth rate, indicating the contribution from organics to particle growth. So the increase of biogenic VOCs could benefit the nucleation and growth of nucleation mode particles at Mt. Yulong.

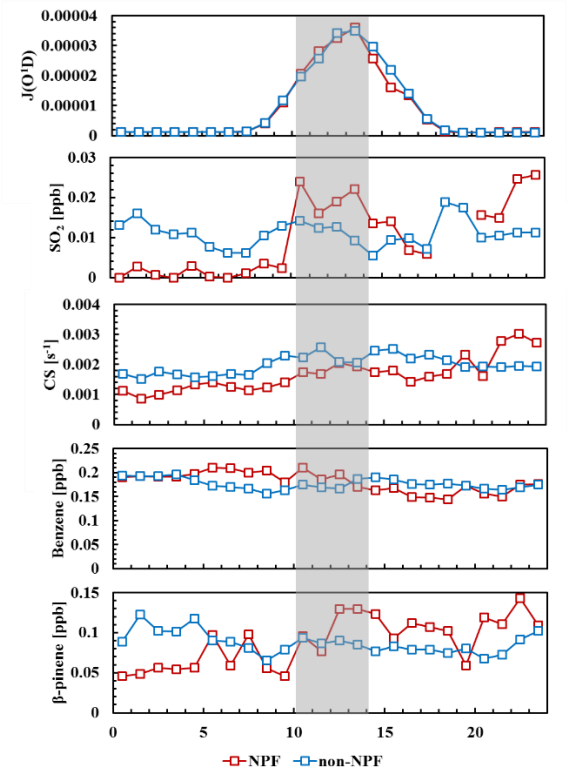

617

618 **Figure 7. Diurnal variation of J(O^1D), SO_2, CS, Benzene, β-pinene during days**
619 **with NPF events (labelled as "NPF", red lines with marks), and without NPF**
620 **events (labelled as "non-NPF", blue lines with marks). Shadow marks the time**
621 **period during which nucleation occurred.**

622

623 3.4.3 Parameters of NPF events ~~at Mt. Yulong~~in this study

624 Formation rate, growth rate and condensation sink of NPF events at Mt. Yulong
625 were summarized in Table 4. Compared with other high mountain measurements, this
626 study reported a higher FR, e.g. 3 times as that at Storm peak laboratory (Hallar et al.,
627 2011). But the GR at Mt. Yulong was within average level, indicating different
628 precursors participating in nucleation and growth process. Even though SO_2 was well
629 correlated with nucleation events, the calculated growth rate by condensation of
630 H_2SO_4 can only explain 5 % of the measured GR. This result indicated participation
631 of some other precursors in particle growth, e.g. organics.

632

633

634 **Table 4. Comparisons of NPF parameters (FR, GR, CS) with the other studies.**

Site	Region	Altitude [m]	Size [nm]	FR [$cm^{-3}s^{-1}$]	GR [nm h^{-1}]	CS [s^{-1}]	Reference
Mt. Yulong	Asia	3410	3-25	1.18~~33~~	3.22	0.002	This research
Mukteshwar	Asia	2180	15-20	0.44	2.47	0.015	(Neitola et al., 2011)
Storm peak laboratory	North America	3210	9-334	0.39	7.5	0.001	(Hallar et al., 2011)
Mt. Tai	Asia	1500	3-25	4	6.1	0.02	(Shen et al., 2016)
Izaña	Atlantic Ocean	2400	10-25	0.46	0.43	0.002	(García et al., 2014)
Jungfraujoch	Europe	3580	3.2-15	1.8	4.0	-	(Tröstl et al., 2016b)
Dome C	Antarctica	3200	10-25	0.023	2.5	0.0002	(Järvinen et al., 2013)

635

636 **4.** Conclusion

637 PNSD, meteorological parameters, trace gases and particle chemical composition
638 were measured at Mt. Yulong site (3410 m a.s.l.) in Southeast corner of Tibet Plateau,
639 during pre-monsoon season (22 March to 15 April) of 2015. PNSD in background
640 atmosphere of Tibet Plateau was characterized. As a background site in Southwest
641 China, the atmosphere of Mt. Yulong exhibited ~~a feature of~~ lower particle level and
642 stronger oxidation capacity ~~,~~than low attitude atmosphere.

643 PBL convection is an influencing factor of PNSD, which caused readable diurnal
644 variation of N_{ait}. Diurnal variation of CO/NO_x and absolute humidity showed that the
645 monitoring site was influenced by PBL during 10:00-14:00, and showed typical FT
646 condition during 1:00-6:00.

647 Three different types of BB event periods were identified by content of BC, *f*60,
648 air mass backward trajectory and fire spot map. Accumulation mode was dominant in
649 transported BB particles from Myanmar, but less aged compared with other Tibet
650 Plateau sites under influence of BB. Under local biomass burning episode, Aitken
651 mode was dominant in PNSD. The biomass burning from South Asia had strong
652 influence on climate parameters, especially for FT. Concentrations of CCN in FT at
653 Mt. Yulong during BB events were 3-9 times as that during BG period. Due to high
654 fraction of organic compounds, the CCN activity of particles in atmosphere of Mt.
655 Yulong was lower than other high altitude sites and ground level sites.

Unexpected low NPF frequency was found in clean atmosphere at Mt. Yulong, due to low concentration of anthropogenic precursor, i.e. SO_2. Occurrence of NPF events were favored by elevated surface emission of SO_2 and transported BB pollutants from South Asia. Off-site NPF event was also observed, during which nanoparticles were formed in PBL and transported to the site. Condensation of sulfuric acid can only explain 5 % of GR in on-site NPF events, indicating other precursors participating in particle growth. NPF can hardly contribute to CCN, since the newly formed particles cannot reach the critical diameter.

Our study provided important dataset ~~in vertical profile~~ of particle~~s~~ physical properties at Tibet Plateau. Influences of BB activities in South Asia and local area on PNSD and CCN in atmosphere of Tibet Plateau were highlighted. Different types of NPF in upper troposphere in Southwest China were characterized, and role of SO_2 were analyzed. Results of our study could be used in regional and global climate model, and help building up the knowledge of NPF in upper part of troposphere.

Acknowledgement

This study was supported by National Natural Science Foundation of China (91544214~~, 41421064~~, 51636003, 21677002), ~~National Key Research and Development Program of China (2016YFC0202000: Task 3),~~ the China Ministry of Environmental Protection Special Funds for Scientific Research on Public Welfare (201309016). We thank Jie Li and Zhangyu Qia from for help with running the WRF model. We also thank the colleagues in the China National Environmental Monitoring Center and Lijiang Monitoring Station for the support to the field campaign.

References

Adak, A.: Atmospheric Fine Mode Particulates at Eastern Himalaya, India: Role of Meteorology, Long-Range Transport and Local Anthropogenic Sources, Aerosol and Air Quality Research, 10.4209/aaqr.2013.03.0090, 2014.

Benajes, J., Garcia, A., Monsalve-Serrano, J., and Boronat, V.: Gaseous emissions and particle size distribution of dual-mode dual-fuel diesel-gasoline concept from low to full load, Applied Thermal Engineering, 120, 138-149, 2017.

Bianchi, F., Tröstl, J., Junninen, H., Frege, C., Henne, S., Hoyle, C. R., Molteni, U., Herrmann, E., Adamov,

688 A., Bukowiecki, N., Chen, X., Duplissy, J., Gysel, M., Hutterli, M., Kangasluoma, J., Kontkanen, J., Kürten,
689 A., Manninen, H. E., Münch, S., Peräkylä, O., Petäjä, T., Rondo, L., Williamson, C., Weingartner, E.,
690 Curtius, J., Worsnop, D. R., Kulmala, M., Dommen, J., and Baltensperger, U.: New particle formation in
691 the free troposphere: A question of chemistry and timing, Science, 352, 1109, 2016.
692 Bonasoni, P., Laj, P., Marinoni, A., Sprenger, M., Angelini, F., Arduini, J., Bonafè, U., Calzolari, F.,
693 Colombo, T., Decesari, S., Di Biagio, C., di Sarra, A. G., Evangelisti, F., Duchi, R., Facchini, M. C., Fuzzi, S.,
694 Gobbi, G. P., Maione, M., Panday, A., Roccato, F., Sellegri, K., Venzac, H., Verza, G. P., Villani, P.,
695 Vuillermoz, E., and Cristofanelli, P.: Atmospheric Brown Clouds in the Himalayas: first two years of
696 continuous observations at the Nepal Climate Observatory-Pyramid (5079 m), Atmos. Chem. Phys., 10,
697 7515-7531, 10.5194/acp-10-7515-2010, 2010.
698 Boy, M., Karl, T., Turnipseed, A., Mauldin, R. L., Kosciuch, E., Greenberg, J., Rathbone, J., Smith, J., Held,
699 A., Barsanti, K., Wehner, B., Bauer, S., Wiedensohler, A., Bonn, B., Kulmala, M., and Guenther, A.: New
700 particle formation in the Front Range of the Colorado Rocky Mountains, Atmos. Chem. Phys., 8,
701 1577-1590, 10.5194/acp-8-1577-2008, 2008.
702 Bukowiecki, N., Weingartner, E., Gysel, M., Coen, M. C., Zieger, P., Herrmann, E., Steinbacher, M.,
703 Gäggeler, H. W., and Baltensperger, U.: A Review of More than 20 Years of Aerosol Observation at the
704 High Altitude Research Station Jungfraujoch, Switzerland (3580 m asl), Aerosol and Air Quality
705 Research, 16, 764-788, 10.4209/aaqr.2015.05.0305, 2016.
706 Cai, R., Yang, D., Fu, Y., Wang, X., Li, X., Ma, Y., Hao, J., Zheng, J., and Jiang, J.: Aerosol Surface Area
707 Concentration: a Governing Factor for New Particle Formation in Beijing, Atmos. Chem. Phys. Discuss.,
708 2017, 1-26, 10.5194/acp-2017-467, 2017.
709 Cerully, K. M., Raatikainen, T., Lance, S., Tkacik, D., Tiitta, P., Petäjä, T., Ehn, M., Kulmala, M., Worsnop,
710 D. R., Laaksonen, A., Smith, J. N., and Nenes, A.: Aerosol hygroscopicity and CCN activation kinetics in
711 a boreal forest environment during the 2007 EUCAARI campaign, Atmospheric Chemistry and Physics,
712 11, 12369-12386, 10.5194/acp-11-12369-2011, 2011.
713 Chen, Y., Cao, J., Zhao, J., Xu, H., Arimoto, R., Wang, G., Han, Y., Shen, Z., and Li, G.: N-alkanes and
714 polycyclic aromatic hydrocarbons in total suspended particulates from the southeastern Tibetan
715 Plateau: concentrations, seasonal variations, and sources, The Science of the total environment,
716 470-471, 9-18, 10.1016/j.scitotenv.2013.09.033, 2014.
717 Cong, Z., Kang, S., Kawamura, K., Liu, B., Wan, X., Wang, Z., Gao, S., and Fu, P.: Carbonaceous aerosols
718 on the south edge of the Tibetan Plateau: concentrations, seasonality and sources, Atmos. Chem.
719 Phys., 15, 1573-1584, 10.5194/acp-15-1573-2015, 2015.
720 Creamean, J. M., Ault, A. P., Ten Hoeve, J. E., Jacobson, M. Z., Roberts, G. C., and Prather, K. A.:
721 Measurements of aerosol chemistry during new particle formation events at a remote rural mountain
722 site, Environmental science & technology, 45, 8208-8216, 10.1021/es103692f, 2011.
723 Cristofanelli, P., Landi, T. C., Calzolari, F., Duchi, R., Marinoni, A., Rinaldi, M., and Bonasoni, P.: Summer
724 atmospheric composition over the Mediterranean basin: Investigation on transport processes and
725 pollutant export to the free troposphere by observations at the WMO/GAW Mt. Cimone global station
726 (Italy, 2165 m a.s.l.), Atmospheric Environment, 141, 139-152, 10.1016/j.atmosenv.2016.06.048, 2016.
727 D'Andrea, S. D., Ng, J. Y., Kodros, J. K., Atwood, S. A., Wheeler, M. J., Macdonald, A. M., Leaitch, W. R.,
728 and Pierce, J. R.: Source attribution of aerosol size distributions and model evaluation using Whistler
729 Mountain measurements and GEOS-Chem-TOMAS simulations, Atmos. Chem. Phys., 16, 383-396,
730 10.5194/acp-16-383-2016, 2016.
731 Dal Maso, M., Kulmala, M., Riipinen, I., Wagner, R., Hussein, T., Aalto, P. P., and Lehtinen, K. E. J.:

Formation and growth of fresh atmospheric aerosols: eight years of aerosol size distribution data from SMEAR II, Hyytiala, Finland, Boreal Environ. Res., 10, 323-336, 2005.
Draxier, R. R., and Hess, G. D.: An overview of the HYSPLIT_4 modelling system for trajectories, dispersion and deposition, Aust. Meteorol. Mag., 47, 295-308, 1998.
Du, W., Sun, Y. L., Xu, Y. S., Jiang, Q., Wang, Q. Q., Yang, W., Wang, F., Bai, Z. P., Zhao, X. D., and Yang, Y. C.: Chemical characterization of submicron aerosol and particle growth events at a national background site (3295 m a.s.l.) on the Tibetan Plateau, Atmos. Chem. Phys., 15, 10811-10824, 10.5194/acp-15-10811-2015, 2015.
Ehhalt, D. H., and Rohrer, F.: Dependence of the OH concentration on solar UV, J Geophys Res-Atmos, 105, 3565-3571, 10.1029/1999jd901070, 2000.
Fröhlich, R., Cubison, M. J., Slowik, J. G., Bukowiecki, N., Canonaco, F., Croteau, P. L., Gysel, M., Henne, S., Herrmann, E., Jayne, J. T., Steinbacher, M., Worsnop, D. R., Baltensperger, U., and Prévôt, A. S. H.: Fourteen months of on-line measurements of the non-refractory submicron aerosol at the Jungfraujoch (3580 m a.s.l.) – chemical composition, origins and organic aerosol sources, Atmos. Chem. Phys., 15, 11373-11398, 10.5194/acp-15-11373-2015, 2015.
García, M. I., Rodríguez, S., González, Y., and García, R. D.: Climatology of new particle formation at Izaña mountain GAW observatory in the subtropical North Atlantic, Atmos. Chem. Phys., 14, 3865-3881, 10.5194/acp-14-3865-2014, 2014.
Gautam, R., Hsu, N. C., Lau, K. M., Tsay, S. C., and Kafatos, M.: Enhanced pre-monsoon warming over the Himalayan-Gangetic region from 1979 to 2007, Geophysical Research Letters, 36, n/a-n/a, 10.1029/2009gl037641, 2009.
Gordon, H., Sengupta, K., Rap, A., Duplissy, J., Frege, C., Williamson, C., Heinritzi, M., Simon, M., Yan, C., Almeida, J., Trostl, J., Nieminen, T., Ortega, I. K., Wagner, R., Dunne, E. M., Adamov, A., Amorim, A., Bernhammer, A. K., Bianchi, F., Breitenlechner, M., Brilke, S., Chen, X. M., Craven, J. S., Dias, A., Ehrhart, S., Fischer, L., Flagan, R. C., Franchin, A., Fuchs, C., Guida, R., Hakala, J., Hoyle, C. R., Jokinen, T., Junninen, H., Kangasluoma, J., Kim, J., Kirkby, J., Krapf, M., Kurten, A., Laaksonen, A., Lehtipalo, K., Makhmutov, V., Mathot, S., Molteni, U., Monks, S. A., Onnela, A., Perakyla, O., Piel, F., Petaja, T., Praplanh, A. P., Pringle, K. J., Richards, N. A. D., Rissanen, M. P., Rondo, L., Sarnela, N., Schobesberger, S., Scott, C. E., Seinfeldo, J. H., Sharma, S., Sipila, M., Steiner, G., Stozhkov, Y., Stratmann, F., Tome, A., Virtanen, A., Vogel, A. L., Wagner, A. C., Wagner, P. E., Weingartner, E., Wimmer, D., Winkler, P. M., Ye, P. L., Zhang, X., Hansel, A., Dommen, J., Donahue, N. M., Worsnop, D. R., Baltensperger, U., Kulmala, M., Curtius, J., and Carslaw, K. S.: Reduced anthropogenic aerosol radiative forcing caused by biogenic new particle formation, Proceedings of the National Academy of Sciences of the United States of America, 113, 12053-12058, 10.1073/pnas.1602360113, 2016.
Guo, H., Wang, D. W., Cheung, K., Ling, Z. H., Chan, C. K., and Yao, X. H.: Observation of aerosol size distribution and new particle formation at a mountain site in subtropical Hong Kong, Atmospheric Chemistry and Physics, 12, 9923-9939, 10.5194/acp-12-9923-2012, 2012.
Gysel, M., Crosier, J., Topping, D. O., Whitehead, J. D., Bower, K. N., Cubison, M. J., Williams, P. I., Flynn, M. J., McFiggans, G. B., and Coe, H.: Closure study between chemical composition and hygroscopic growth of aerosol particles during TORCH2, Atmos. Chem. Phys., 7, 6131-6144, 10.5194/acp-7-6131-2007, 2007.
Hallar, A. G., Lowenthal, D. H., Chirokova, G., Borys, R. D., and Wiedinmyer, C.: Persistent daily new particle formation at a mountain-top location, Atmospheric Environment, 45, 4111-4115, 10.1016/j.atmosenv.2011.04.044, 2011.

776 Harris, S., and Maricq, M. M.: Signature size distributions for diesel and gasoline engine exhaust
777 particulate matter, 749-764 pp., 2001.
778 Herrmann, E., Weingartner, E., Henne, S., Vuilleumier, L., Bukowiecki, N., Steinbacher, M., Conen, F.,
779 Collaud Coen, M., Hammer, E., Jurányi, Z., Baltensperger, U., and Gysel, M.: Analysis of long-term
780 aerosol size distribution data from Jungfraujoch with emphasis on free tropospheric conditions, cloud
781 influence, and air mass transport, Journal of Geophysical Research: Atmospheres, 120, 9459-9480,
782 10.1002/2015jd023660, 2015.
783 Huang, X., Zhou, L., Ding, A., Qi, X., Nie, W., Wang, M., Chi, X., Petäjä, T., Kerminen, V. M., Roldin, P.,
784 Rusanen, A., Kulmala, M., and Boy, M.: Comprehensive modelling study on observed new particle
785 formation at the SORPES station in Nanjing, China, Atmos. Chem. Phys., 16, 2477-2492,
786 10.5194/acp-16-2477-2016, 2016.
787 Hussein, T., Dal Maso, M., Petaja, T., Koponen, I. K., Paatero, P., Aalto, P. P., Hameri, K., and Kulmala, M.:
788 Evaluation of an automatic algorithm for fitting the particle number size distributions, Boreal Environ.
789 Res., 10, 337-355, 2005.
790 Järvinen, E., Virkkula, A., Nieminen, T., Aalto, P. P., Asmi, E., Lanconelli, C., Busetto, M., Lupi, A.,
791 Schioppo, R., Vitale, V., Mazzola, M., Petäjä, T., Kerminen, V. M., and Kulmala, M.: Seasonal cycle and
792 modal structure of particle number size distribution at Dome C, Antarctica, Atmospheric Chemistry
793 and Physics, 13, 7473-7487, 10.5194/acp-13-7473-2013, 2013.
794 Jaeglé, L., Jacob, D. J., Wang, Y., Weinheimer, A. J., Ridley, B. A., Campos, T. L., Sachse, G. W., and
795 Hagen, D. E.: Sources and chemistry of NOxin the upper troposphere over the United States,
796 Geophysical Research Letters, 25, 1705-1708, 10.1029/97gl03591, 1998.
797 Kittelson, D. B., Watts, W. F., and Johnson, J. P.: On-road and laboratory evaluation of combustion
798 aerosols—Part1: Summary of diesel engine results, Journal of Aerosol Science, 37, 913-930,
799 https://doi.org/10.1016/j.jaerosci.2005.08.005, 2006.
800 Kivekäs, N., Sun, J., Zhan, M., Kerminen, V. M., Hyvärinen, A., Komppula, M., Viisanen, Y., Hong, N.,
801 Zhang, Y., Kulmala, M., Zhang, X. C., Deli, G., and Lihavainen, H.: Long term particle size distribution
802 measurements at Mount Waliguan, a high-altitude site in inland China, Atmos. Chem. Phys., 9,
803 5461-5474, 10.5194/acp-9-5461-2009, 2009.
804 Komppula, M., Lihavainen, H., Hyvärinen, A. P., Kerminen, V. M., Panwar, T. S., Sharma, V. P., and
805 Viisanen, Y.: Physical properties of aerosol particles at a Himalayan background site in India, Journal of
806 Geophysical Research, 114, 10.1029/2008jd011007, 2009.
807 Kulmala, M., maso, M. D., Mäkelä, J. M., Pirjola, L., Väkevä, M., Aalto, P., Miikkulainen, P., Hämeri, K.,
808 #039, and dowd, C. D.: On the formation, growth and composition of nucleation mode particles, 2001,
809 53, 10.3402/tellusb.v53i4.16622, 2001.
810 Lüthi, Z. L., Škerlak, B., Kim, S. W., Lauer, A., Mues, A., Rupakheti, M., and Kang, S.: Atmospheric brown
811 clouds reach the Tibetan Plateau by crossing the Himalayas, Atmos. Chem. Phys., 15, 6007-6021,
812 10.5194/acp-15-6007-2015, 2015.
813 Laing, J. R., Jaffe, D. A., and Hee, J. R.: Physical and optical properties of aged biomass burning aerosol
814 from wildfires in Siberia and the Western USA at the Mt. Bachelor Observatory, Atmos. Chem. Phys.,
815 16, 15185-15197, 10.5194/acp-16-15185-2016, 2016.
816 Lathem, T. L., Beyersdorf, A. J., Thornhill, K. L., Winstead, E. L., Cubison, M. J., Hecobian, A., Jimenez, J.
817 L., Weber, R. J., Anderson, B. E., and Nenes, A.: Analysis of CCN activity of Arctic aerosol and Canadian
818 biomass burning during summer 2008, Atmospheric Chemistry and Physics, 13, 2735-2756,
819 10.5194/acp-13-2735-2013, 2013.

Lunden, M. M., Black, D. R., McKay, M., Revzan, K. L., Goldstein, A. H., and Brown, N. J.: Characteristics of Fine Particle Growth Events Observed Above a Forested Ecosystem in the Sierra Nevada Mountains of California, Aerosol Science and Technology, 40, 373-388, 10.1080/02786820600631896, 2006.
Merikanto, J., Spracklen, D. V., Mann, G. W., Pickering, S. J., and Carslaw, K. S.: Impact of nucleation on global CCN, Atmospheric Chemistry And Physics, 9, 8601-8616, 10.5194/acp-9-8601-2009, 2009.
Neitola, K., Asmi, E., Komppula, M., Hyvärinen, A. P., Raatikainen, T., Panwar, T. S., Sharma, V. P., and Lihavainen, H.: New particle formation infrequently observed in Himalayan foothills – why?, Atmospheric Chemistry and Physics, 11, 8447-8458, 10.5194/acp-11-8447-2011, 2011.
Nishita, C., Osada, K., Kido, M., Matsunaga, K., and Iwasaka, Y.: Nucleation mode particles in upslope valley winds at Mount Norikura, Japan: Implications for the vertical extent of new particle formation events in the lower troposphere, Journal of Geophysical Research, 113, 10.1029/2007jd009302, 2008.
Okamoto, S., and Tanimoto, H.: A review of atmospheric chemistry observations at mountain sites, Progress in Earth and Planetary Science, 3, 10.1186/s40645-016-0109-2, 2016.
Peng, J. F., Hu, M., Wang, Z. B., Huang, X. F., Kumar, P., Wu, Z. J., Guo, S., Yue, D. L., Shang, D. J., Zheng, Z., and He, L. Y.: Submicron aerosols at thirteen diversified sites in China: size distribution, new particle formation and corresponding contribution to cloud condensation nuclei production, Atmospheric Chemistry and Physics, 14, 10249-10265, 10.5194/acp-14-10249-2014, 2014.
Petters, M. D., and Kreidenweis, S. M.: A single parameter representation of hygroscopic growth and cloud condensation nucleus activity, Atmos. Chem. Phys., 7, 1961-1971, 10.5194/acp-7-1961-2007, 2007.
Pierce, J. R., Leaitch, W. R., Liggio, J., Westervelt, D. M., Wainwright, C. D., Abbatt, J. P. D., Ahlm, L., Al-Basheer, W., Cziczo, D. J., Hayden, K. L., Lee, A. K. Y., Li, S. M., Russell, L. M., Sjostedt, S. J., Strawbridge, K. B., Travis, M., Vlasenko, A., Wentzell, J. J. B., Wiebe, H. A., Wong, J. P. S., and Macdonald, A. M.: Nucleation and condensational growth to CCN sizes during a sustained pristine biogenic SOA event in a forested mountain valley, Atmos. Chem. Phys., 12, 3147-3163, 10.5194/acp-12-3147-2012, 2012.
Rodríguez, S., González, Y., Cuevas, E., Ramos, R., Romero, P. M., Abreu-Afonso, J., and Redondas, A.: Atmospheric nanoparticle observations in the low free troposphere during upward orographic flows at Izaña Mountain Observatory, Atmos. Chem. Phys., 9, 6319-6335, 10.5194/acp-9-6319-2009, 2009.
Rose, C., Sellegri, K., Freney, E., Dupuy, R., Colomb, A., Pichon, J. M., Ribeiro, M., Bourianne, T., Burnet, F., and Schwarzenboeck, A.: Airborne measurements of new particle formation in the free troposphere above the Mediterranean Sea during the HYMEX campaign, Atmospheric Chemistry and Physics, 15, 10203-10218, 10.5194/acp-15-10203-2015, 2015.
Shen, X., Sun, J., Zhang, X., Kivekäs, N., Zhang, Y., Wang, T., Zhang, X., Yang, Y., Wang, D., Zhao, Y., and Qin, D.: Particle Climatology in Central East China Retrieved from Measurements in Planetary Boundary Layer and in Free Troposphere at a 1500-m-High Mountaintop Site, Aerosol and Air Quality Research, 16, 659-701, 10.4209/aaqr.2015.02.0070, 2016.
Shen, X. J., Sun, J. Y., Zhang, Y. M., Wehner, B., Nowak, A., Tuch, T., Zhang, X. C., Wang, T. T., Zhou, H. G., Zhang, X. L., Dong, F., Birmili, W., and Wiedensohler, A.: First long-term study of particle number size distributions and new particle formation events of regional aerosol in the North China Plain, Atmospheric Chemistry and Physics, 11, 1565-1580, 10.5194/acp-11-1565-2011, 2011.
Sipilä, M., Berndt, T., Petäjä, T., Brus, D., Vanhanen, J., Stratmann, F., Patokoski, J., Mauldin, R. L., Hyvärinen, A.-P., Lihavainen, H., and Kulmala, M.: The Role of Sulfuric Acid in Atmospheric Nucleation, Science, 327, 1243-1246, 10.1126/science.1180315, 2010.

Tan, P. Q., Li, Y., Hu, Z. Y., and Lou, D. M.: Investigation of nitrogen oxides, particle number, and size distribution on a light-duty diesel car with B10 and G10 fuels, Fuel, 197, 373-387, 2017.

Tröstl, J., Chuang, W. K., Gordon, H., Heinritzi, M., Yan, C., Molteni, U., Ahlm, L., Frege, C., Bianchi, F., Wagner, R., Simon, M., Lehtipalo, K., Williamson, C., Craven, J. S., Duplissy, J., Adamov, A., Almeida, J., Bernhammer, A.-K., Breitenlechner, M., Brilke, S., Dias, A., Ehrhart, S., Flagan, R. C., Franchin, A., Fuchs, C., Guida, R., Gysel, M., Hansel, A., Hoyle, C. R., Jokinen, T., Junninen, H., Kangasluoma, J., Keskinen, H., Kim, J., Krapf, M., Kürten, A., Laaksonen, A., Lawler, M., Leiminger, M., Mathot, S., Möhler, O., Nieminen, T., Onnela, A., Petäjä, T., Piel, F. M., Miettinen, P., Rissanen, M. P., Rondo, L., Sarnela, N., Schobesberger, S., Sengupta, K., Sipilä, M., Smith, J. N., Steiner, G., Tomè, A., Virtanen, A., Wagner, A. C., Weingartner, E., Wimmer, D., Winkler, P. M., Ye, P., Carslaw, K. S., Curtius, J., Dommen, J., Kirkby, J., Kulmala, M., Riipinen, I., Worsnop, D. R., Donahue, N. M., and Baltensperger, U.: The role of low-volatility organic compounds in initial particle growth in the atmosphere, Nature, 533, 527-531, 10.1038/nature18271, 2016a.

Tröstl, J., Herrmann, E., Frege, C., Bianchi, F., Molteni, U., Bukowiecki, N., Hoyle, C. R., Steinbacher, M., Weingartner, E., Dommen, J., Gysel, M., and Baltensperger, U.: Contribution of new particle formation to the total aerosol concentration at the high-altitude site Jungfraujoch (3580 m asl, Switzerland), Journal of Geophysical Research: Atmospheres, 121, 11,692-611,711, 10.1002/2015jd024637, 2016b.

Vu, T. V., Delgado-Saborit, J. M., and Harrison, R. M.: Review: Particle number size distributions from seven major sources and implications for source apportionment studies, Atmospheric Environment, 122, 114-132, 2015.

Wang, Z., Wu, Z., Yue, D., Shang, D., Guo, S., Sun, J., Ding, A., Wang, L., Jiang, J., Guo, H., Gao, J., Cheung, H. C., Morawska, L., Keywood, M., and Hu, M.: New particle formation in China: Current knowledge and further directions, The Science of the total environment, 577, 258-266, 10.1016/j.scitotenv.2016.10.177, 2017.

Wang, Z. B., Hu, M., Yue, D. L., Zheng, J., Zhang, R. Y., Wiedensohler, A., Wu, Z. J., Nieminen, T., and Boy, M.: Evaluation on the role of sulfuric acid in the mechanisms of new particle formation for Beijing case, Atmospheric Chemistry and Physics, 11, 12663-12671, 10.5194/acp-11-12663-2011, 2011.

Wang, Z. B., Hu, M., Sun, J. Y., Wu, Z. J., Yue, D. L., Shen, X. J., Zhang, Y. M., Pei, X. Y., Cheng, Y. F., and Wiedensohler, A.: Characteristics of regional new particle formation in urban and regional background environments in the North China Plain, Atmospheric Chemistry and Physics, 13, 12495-12506, 10.5194/acp-13-12495-2013, 2013a.

Wang, Z. B., Hu, M., Wu, Z. J., Yue, D. L., He, L. Y., Huang, X. F., Liu, X. G., and Wiedensohler, A.: Long-term measurements of particle number size distributions and the relationships with air mass history and source apportionment in the summer of Beijing, Atmospheric Chemistry and Physics, 13, 10159-10170, 10.5194/acp-13-10159-2013, 2013b.

Weller, R., Schmidt, K., Teinilä, K., and Hillamo, R.: Natural new particle formation at the coastal Antarctic site Neumayer, Atmospheric Chemistry and Physics, 15, 11399-11410, 10.5194/acp-15-11399-2015, 2015.

Wu, Z., Hu, M., Liu, S., Wehner, B., Bauer, S., Ma ßling, A., Wiedensohler, A., Petäjä, T., Dal Maso, M., and Kulmala, M.: New particle formation in Beijing, China: Statistical analysis of a 1-year data set, Journal of Geophysical Research, 112, 10.1029/2006jd007406, 2007.

Wu, Z., Hu, M., Lin, P., Liu, S., Wehner, B., and Wiedensohler, A.: Particle number size distribution in the urban atmosphere of Beijing, China, Atmospheric Environment, 42, 7967-7980, 10.1016/j.atmosenv.2008.06.022, 2008.

Wu, Z. J., Poulain, L., Henning, S., Dieckmann, K., Birmili, W., Merkel, M., van Pinxteren, D., Spindler, G., Müller, K., Stratmann, F., Herrmann, H., and Wiedensohler, A.: Relating particle hygroscopicity and CCN activity to chemical composition during the HCCT-2010 field campaign, Atmos. Chem. Phys., 13, 7983-7996, 10.5194/acp-13-7983-2013, 2013.

Wu, Z. J., Zheng, J., Shang, D. J., Du, Z. F., Wu, Y. S., Zeng, L. M., Wiedensohler, A., and Hu, M.: Particle hygroscopicity and its link to chemical composition in the urban atmosphere of Beijing, China, during summertime, Atmos. Chem. Phys., 16, 1123-1138, 10.5194/acp-16-1123-2016, 2016.

Xu, J., Wang, Z., Yu, G., Qin, X., Ren, J., and Qin, D.: Characteristics of water soluble ionic species in fine particles from a high altitude site on the northern boundary of Tibetan Plateau: Mixture of mineral dust and anthropogenic aerosol, Atmospheric Research, 143, 43-56, 10.1016/j.atmosres.2014.01.018, 2014.

Xu, J. Z., Zhang, Q., Wang, Z. B., Yu, G. M., Ge, X. L., and Qin, X.: Chemical composition and size distribution of summertime PM2.5 at a high altitude remote location in the northeast of the Qinghai–Xizang (Tibet) Plateau: insights into aerosol sources and processing in free troposphere, Atmospheric Chemistry and Physics, 15, 5069-5081, 10.5194/acp-15-5069-2015, 2015.

Yli-Juuti, T., Riipinen, I., Aalto, P. P., Nieminen, T., Maenhaut, W., Janssens, I. A., Claeys, M., Salma, I., Ocskay, R., Hoffer, A., Imre, K., and Kulmala, M.: Characteristics of new particle formation events and cluster ions at K-puszta, Hungary, Boreal Environ. Res., 14, 683-698, 2009.

Yu, F., and Hallar, A. G.: Difference in particle formation at a mountaintop location during spring and summer: Implications for the role of sulfuric acid and organics in nucleation, Journal of Geophysical Research: Atmospheres, 119, 12,246-212,255, 10.1002/2014jd022136, 2014.

Yue, D. L., Hu, M., Zhang, R. Y., Wang, Z. B., Zheng, J., Wu, Z. J., Wiedensohler, A., He, L. Y., Huang, X. F., and Zhu, T.: The roles of sulfuric acid in new particle formation and growth in the mega-city of Beijing, Atmospheric Chemistry And Physics, 10, 4953-4960, 10.5194/acp-10-4953-2010, 2010.

Zellweger, C., Forrer, J., Hofer, P., Nyeki, S., Schwarzenbach, B., Weingartner, E., Ammann, M., and Baltensperger, U.: Partitioning of reactive nitrogen (NOy) and dependence on meteorological conditions in the lower free troposphere, Atmos. Chem. Phys., 3, 779-796, 10.5194/acp-3-779-2003, 2003.

Zhang, R., Khalizov, A., Wang, L., Hu, M., and Xu, W.: Nucleation and growth of nanoparticles in the atmosphere, Chemical reviews, 112, 1957-2011, 10.1021/cr2001756, 2012.

Zhang, X., Yin, Y., Lin, Z., Han, Y., Hao, J., Yuan, L., Chen, K., Chen, J., Kong, S., Shan, Y., Xiao, H., and Tan, W.: Observation of aerosol number size distribution and new particle formation at a mountainous site in Southeast China, The Science of the total environment, 575, 309-320, 10.1016/j.scitotenv.2016.09.212, 2016.

Zheng, J., Hu, M., Peng, J., Wu, Z., Kumar, P., Li, M., Wang, Y., and Guo, S.: Spatial distributions and chemical properties of PM2.5 based on 21 field campaigns at 17 sites in China, Chemosphere, 159, 480-487, 10.1016/j.chemosphere.2016.06.032, 2016.

Zheng, J., Hu, M., Du, Z., Shang, D., Gong, Z., Qin, Y., Fang, J., Gu, F., Li, M., Peng, J., Li, J., Zhang, Y., Huang, X., He, L., Wu, Y., and Guo, S.: Influence of biomass burning from South Asia at a high-altitude mountain receptor site in China, Atmos. Chem. Phys., 17, 6853-6864, 10.5194/acp-17-6853-2017, 2017.